Dynamics and thermodynamics of crystalline polymorphs. 3. -glycine, analysis of variable-temperature atomic displacement parameters, and comparison of polymorph stabilities

Aree, Thammarat ; Bürgi, Hans-Beat ; Chernyshov, Dmitry ; Törnroos, Karl W

Abstract: In a series of systematic studies, we have investigated the molecular motion in crystals of the glycine polymorphs and determined their thermodynamic functions from an analysis of multitemperature atomic displacement parameters (ADPs) combined with ONIOM calculation on 15-molecule clusters. The studies are aimed at providing insight into the factors governing the relative stabilities of the - , -, and -polymorphs. This Article, the last in the series, focuses on the most stable polymorph, -glycine. Multitemperature diffraction data of the -glycine polymorph have been collected to 0.5 Å resolution between 10 and 300 K at two synchrotron beamlines, KEK Photon Factory and ID11 of the ESRF. The ADPs of -glycine from these sources differ significantly, as previously observed also for the other two polymorphs. A simple model of rigid body motion explains the ADPs from KEK and their temperature dependence. It provides lattice vibration frequencies that are in line with those from Raman spectroscopy. Together with the internal vibration frequencies from an ONIOM calculation, the thermodynamic functions are estimated using the Einstein, Debye, and Nernst–Lindemann models of heat capacity. The relative stabilities of the three polymorphs of glycine are discussed on the basis of the contributions to their free energies as obtained in this work and from various experimental and theoretical studies. The comparison shows that the free-energy differences are determined primarily by differences in lattice and zero-point vibrational energies.

DOI: https://doi.org/10.1021/jp506659c

Dynamics and Thermodynamics of Crystalline Polymorphs. 3. γ-Glycine, Analysis of Variable-Temperature Atomic Displacement Parameters and Comparison of Polymorph Stabilities

Thammarat Aree,[1,*] Hans-Beat Bürgi,[2] Dmitry Chernyshov,[3] and Karl W. Törnroos[4]

[1]*Department of Chemistry, Faculty of Science, Chulalongkorn University, Bangkok 10330, Thailand;* [2]*Department of Chemistry and Biochemistry, University of Berne, CH-3012 Bern, and Department of Chemistry, University of Zürich, CH-8050 Zürich, Switzerland;* [3]*Swiss-Norwegian Beam Lines at the European Synchrotron Radiation Facility, France;* [4]*Department of Chemistry, University of Bergen, N-5007 Bergen, Norway*

* Corresponding author. Tel.: + 66-2-2187584. Fax: + 66-2-2187598.

E-mail: thammarat.aree@gmail.com

Abstract

In a series of systematic studies we have investigated the molecular motion in crystals of the glycine polymorphs and determined their thermodynamic functions from an analysis of multi-temperature atomic displacement parameters (ADPs) combined with ONIOM calculation on 15-molecule clusters. The studies are aimed at providing insight into the factors governing the relative stabilities of the α-, β- and γ-polymorphs. This paper, the last in the series, focuses on the most stable polymorph, γ-glycine. Multitemperature diffraction data to 0.5 Å of the γ-glycine polymorph have been collected between 10 and 300 K at two synchrotron beamlines, KEK Photon Factory and ID11 of the ESRF. The ADPs of γ-glycine from these sources differ significantly, as previously observed also for the other two polymorphs. A simple model of rigid body motion explains the ADPs from KEK and their temperature dependence. It provides lattice vibration frequencies that are in line with those from Raman spectroscopy. Together with the internal vibration frequencies from an ONIOM calculation, the thermodynamic functions are estimated using the Einstein, Debye and Nernst–Lindemann models of heat capacity. The relative stabilities of the three polymorphs of glycine are discussed on the basis of the contributions to their free energies as obtained in this work and from various experimental and theoretical studies. The comparison shows that the free-energy differences are determined primarily by differences in lattice and zero-point vibrational energies.

Keywords: γ-glycine; molecular motion; normal mode analysis; atomic displacement parameters, thermodynamics

1. INTRODUCTION

Zwitterionic glycine ($^{+}NH_3CH_2CO_2^{-}$) forms three polymorphs at ambient pressure with relative stabilities and space groups: $\gamma - P3_1 > \alpha - P2_1/n > \beta - P2_1$.[1] Their crystal packings are characterized by parallel polar layers, polar helices, and antiparallel bilayers, respectively. The β- and γ-phases exhibit piezoelectric properties,[2,3] whereas the α-phase shows electrical properties.[4]

This and two preceding papers aim at understanding the various contributions to the thermodynamic functions of the three glycine polymorphs and thus their relative stabilities, the contributions of vibrational enthalpy and entropy in particular. Here these functions are obtained by determining external and internal vibration frequencies[5–7] from the temperature dependence of atomic displacement parameters (ADPs).[8] In this third paper, we report a normal mode analysis of the ADPs of γ-glycine obtained from synchrotron data, derive the relevant thermodynamic functions, and compare the contributions to the relative stabilities of the three glycine polymorphs as obtained from ADPs, calorimetric and theoretical methods. A similar study, in particular an accurate estimation of the heat capacities C_v and C_p using the Einstein,[9] Debye[10] and Nernst–Lindemann[11] relations has been performed for naphthalene, anthracene and hexamethylenetetramine.[12]

A set of multitemperature ADPs may be analysed with the normal mode model developed by Bürgi and Capelli:[8]

$$\boldsymbol{\Sigma}^{\boldsymbol{x}}(T) = \boldsymbol{AgV\delta}(T)\boldsymbol{V}^{\boldsymbol{T}}\boldsymbol{g}^{\boldsymbol{T}}\boldsymbol{A}^{\boldsymbol{T}} + \boldsymbol{\varepsilon}^{\boldsymbol{x}} \qquad (1)$$

The ADPs are the 3×3 diagonal blocks of $\boldsymbol{\Sigma}^{\boldsymbol{x}}$; $\boldsymbol{\delta}(T)$ is a diagonal matrix of temperature-dependent normal mode displacements with elements

$$\delta_i(T) = \frac{h}{8\pi^2\nu_i}\coth\left(\frac{h\nu_i}{2k_BT}\right) \qquad (2)$$

The matrices $\boldsymbol{g}$ and $\boldsymbol{A}$ transform the normal modes with frequencies ν_i and eigenvectors $\boldsymbol{V}$ into mean square atomic displacements $\boldsymbol{\Sigma}^{\boldsymbol{x}}(T)$; $\boldsymbol{\varepsilon}^{\boldsymbol{x}}$ is a temperature-independent term accounting for the high-frequency intramolecular vibrations, which are not significantly excited in the temperature range of the diffraction experiments; h is the Planck constant; and k_B is the Boltzmann constant. The dynamics of the molecules in the crystal field are parameterized by the frequencies ν_i, the independent elements of the orthonormal matrix $\boldsymbol{V}$ representing molecular displacement coordinates and the six independent elements of each of the 3×3 diagonal blocks of $\boldsymbol{\varepsilon}^{\boldsymbol{x}}$. Anharmonicity associated with the thermal expansion of the crystal is taken into account by a Grüneisen parameter[13] (eq. 3) defined as the ratio of the relative

frequency change $\Delta\nu(T)/\nu(0)$ to the relative cell-volume change $\Delta V(T)/V(0)$ with temperature.[14]

$$\gamma_{G,i} = -\frac{V(0)}{\Delta V(T)} \cdot \frac{\Delta \nu_i(T)}{\nu_i(0)} \tag{3}$$

The model parameters are obtained from a least squares procedure with observational equations based on the elements of the diagonal 3×3 blocks of $\boldsymbol{\Sigma}^{\mathbf{x}}(T)$ determined at multiple temperatures (eq. 1).

At atmospheric pressure γ-glycine is the most stable polymorph and has been as extensively studied as α-glycine. The γ-glycine crystal structure was first determined by Iitaka in 1958 using photographic techniques.[15] Kozhin reported the unit cell constants at 77 and 293 K of the three glycine polymorphs in a study of thermal expansion tensors.[16] Kvick and co-workers analyzed thermal motion upon cooling from 298 to 83 K using neutron diffraction data to 0.67 Å resolution.[17] Boldyreva and co-workers measured two sealed-tube X-ray data sets of γ-glycine to a resolution of 0.6 Å using modern CCD diffractometers and studied structural distortions upon cooling from 294 to 150 K.[18] However, these data do not cover the temperature range from the quantum to the classic regimes nor do they extend to a resolution of 0.5 Å, ranges one would like to have for the normal mode analysis described in this communication. In addition, highly intense synchrotron radiation with its small energy dispersion ($\Delta\lambda/\lambda < 10^{-4}$) can help to measure the rather weak Bragg intensities at high angles accurately and thus to obtain accurate ADPs.[19] Due to the small dispersion of synchrotron radiation ADPs are generally smaller by $\sim 6\times10^{-4}$ Å^2 than those obtained from sealed tube radiation.[19]

2. DIFFRACTION EXPERIMENTS

2.1. Crystal Preparation. White powder of glycine purchased from MP Biochemicals was used as received. Elongated trigonal, colorless single crystals of the γ-glycine polymorph were obtained from a saturated acetic acid aqueous solution of glycine by adding (2% w/w of glycine) of *D*-/*L*-phenylalanine as described in (20).

2.2. Data Collection and Processing. Elongated trigonal γ-glycine single crystals were cut, if necessary, to optimal sizes of 0.04–0.25 mm and glued on a glass fiber tip. Synchrotron data for a crystal of γ-glycine were collected to a resolution of 0.5 Å at 10, 70, 130, and 190 K on beamline 8B of KEK Photon Factory (PF) with a wavelength of 0.65210 Å, using an imaging plate Weissenberg camera, on a 2-circle diffractometer. At 298 K, data were

collected on the same beamline to the same resolution using two orientations of a second crystal for better coverage and redundancy. A third crystal was used for data collection at 10, 100, 200 and 300 K with a wavelength of 0.15927 Å and using a 3-circle diffractometer and homemade CCD detector at beamline ID11 of the European Synchrotron Radiation Facility (ESRF) (see Supporting Information, Table 1S). Note that in multi-temperature studies, like the present investigations of the glycine polymorphs,[5–7] it is practically unavoidable to collect diffraction data from different crystal samples at different beamlines and synchrotron sources, in different sample environments and data processing. While this complicates ADP comparisons, it is also allows tests of mutual consistency or discrepancy of the results. Data were processed with RAPID AUTO[21] or SAINT[22] and multi-scan absorption corrections were applied with ABSCOR[23] or SADABS,[24] giving the following completeness, redundancy and R_{int}: 90–99%, 2.0–2.8 and 0.027–0.041 for the KEK data and 98%, 18.9–25.6 and 0.034–0.038 for the ID11 data (Tables 2S). The unit cell dimensions from both sources agree well with each other and with those from sealed tube experiments (Fig. 1S).[18] The intensity data were scaled and merged using XPREP.[25] The structures were determined using SHELXS97[26] and refined with SHELXL97.[26] After refinement of the KEK data between 10–190 K, all reflections showed $F_o^2 >> F_c^2$, indicating that the data were collected from a merohedrally twinned crystal (probably induced by cutting). Hence, the KEK low-temperature data were detwinned prior to multipole refinement (Table 2S, footnote a). The 298 K data from KEK and all data from ID11 collected with two different crystals show no indication of twinning. All non-H atoms were refined anisotropically using conventional spherical scattering factors[27] (Independent Atom Model, IAM). Hydrogen atoms found from difference Fourier maps were refined isotropically. An extinction correction was refined, but was insignificant for the ID11 data (Table 1). This observation correlates with the much shorter wavelength used for data collection at beamline ID11 (Table 1). Inspection of plots of F_{obs}^2 vs F_{calc}^2 for the KEK data showed only one affected reflection ((–1 2 0), see SI, Fig. 2S). ADPs from refinements with and without extinction correction and with and without this reflection differ insignificantly, becoming 0.5 standard uncertainties smaller on average if no extinction correction is considered or the reflection (–1 2 0) omitted from the refinement. Overall extinction was found much less serious than reported for the neutron diffraction data of γ-glycine,[17] probably because the crystal volumes used here (4–0.2 μm^3) are four orders of magnitude smaller than the one used in the neutron study (22.5 mm^3!). The final R_1 values [$I > 2\sigma(I)$] are: 0.033–0.045 for the KEK and 0.022–0.035 for the ID11 data (Tables 1 and 2S). PEANUT[28] plots depicting the temperature evolution of the γ-glycine ADPs obtained from the KEK data are

given in Fig. 1. The ADPs from KEK and ID11 data are compared for atoms C1 and O1 in Fig. 2.

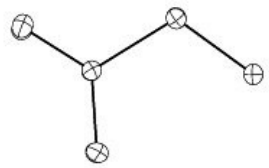

10 K

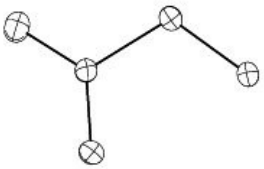

70 K

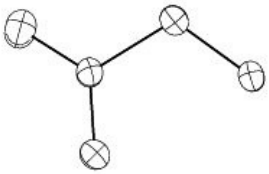

130 K

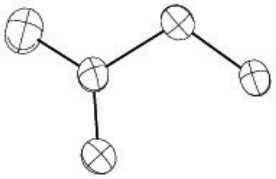

190 K

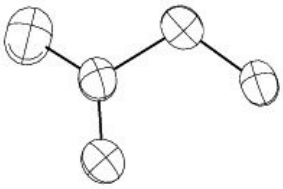

298 K

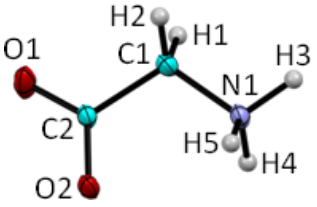

Figure 1. PEANUT[28] plots (rmsd, scale 2.50) of the γ-glycine ADPs derived from KEK data (IAM refinement). The H-atoms are omitted for clarity. The molecule at the bottom right shows the atomic labeling.

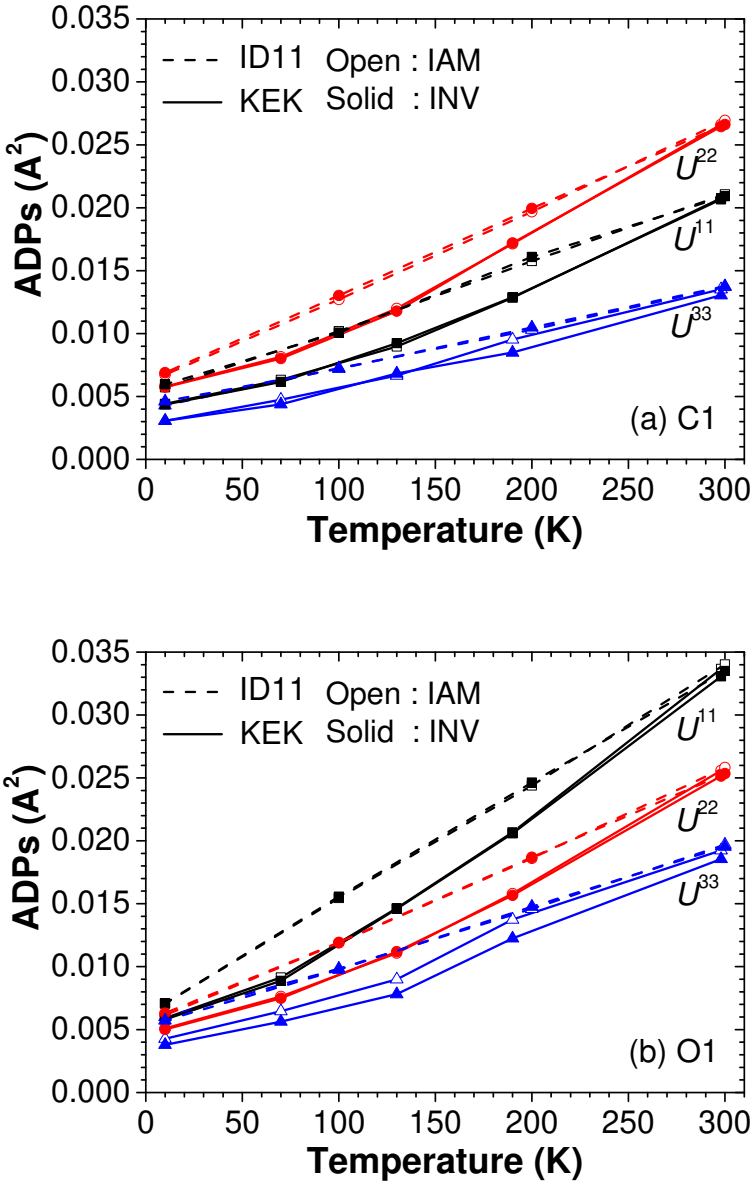

Figure 2. The variable-temperature ADPs of γ-glycine for atoms (a) C1 and (b) O1 from KEK and ID11 data; comparison of ADPs from IAM and INV refinements. The standard uncertainties are 2×10^{-4} Å^2, or ca. the line thickness.

2.3. Deconvolution of Thermal Motion from Valence Bonding Density. ADPs of the non-H atoms minimally biased by directional valence bonding density may be obtained by refining the diffraction data using a multipole model with program XD.[29] We employed the invariom model[30] which has been used successfully for refining the α- and β-glycine data.[5–7] The model is based on the approximation that a non-spherical electron density fragment is invariant in related molecules and that the multipole population parameters are therefore transferable. This treatment generally provides well-defined deformation electron density

maps and improves *R*-values by ~1% as originally observed for MoKα data sets of organic molecules.[31] Here the values of R_1 and $\Delta\rho$ after invariom refinement remain basically unchanged for both the KEK and ID11 data (Table 1). As for the ADPs, the principal elements U^{33} from the KEK data decrease by 4–6 times their standard uncertainties at the higher temperatures, while the other U^{ii} as well as all U^{ii} from the ID11 data remain unchanged (Fig. 2). The differences of mean square displacements along interatomic vectors of bonded non-H atoms are $<1.0\times10^{-3}$ Å^2 for all temperatures, thus satisfying the Hirshfeld's rigid-bond test[32] and warranting the quality of the ADPs obtained.

Table 1. Refinement Statistics for γ-glycine from the Independent Atom Model (IAM) using SHELXL97[26] and from the Invariom Multipole Model (INV) using XD.[29] Data from KEK and ID11

Temp (K)	No of reflns ($>2\sigma$)	EXTI [a]	$R_1(F)$_IAM [b]	$R_1(F)$_INV [b]	$\Delta\rho$_IAM (e Å^{-3})	$\Delta\rho$_INV (e Å^{-3})
KEK						
10	1147	0.04(7)	0.045	0.045	0.62/–0.54	0.49/–0.51
70	1154	0.24(8)	0.037	0.039	0.44/–0.49	0.45/–0.58
130	1152	0.21(7)	0.033	0.032	0.35/–0.48	0.38/–0.49
190	1108	0.19(8)	0.040	0.042	0.36/–0.41	0.35/–0.43
298	1186	0.13(6)	0.037	0.041	0.29/–0.30	0.28/–0.35
ID11						
10	1192	0.00(4)	0.025	0.025	0.37/–0.44	0.33/–0.30
100	1190	0.00(4)	0.022	0.022	0.36/–0.29	0.29/–0.30
200	1188	0.00(5)	0.026	0.026	0.35/–0.27	0.27/–0.28
300	1196	0.00(5)	0.035	0.037	0.35/–0.26	0.28/–0.26

[a] Extinction parameter (x), where F_c is multiplied by: $k[1 + 0.001xF_c^2\lambda^3/\sin(2\theta)]^{-1/4}$
[b] $R_1(F) = \sum||F_o| - |F_c||/\sum|F_o|$.

3. THEORETICAL CALCULATIONS

Whereas glycine exists in its neutral form in the gas phase, the crystal field stabilizes its zwitterionic form. For the theoretical calculations the crystal field was modeled with a 15-molecule cluster comprising a central molecule surrounded by 14 neighbors. The cluster size agrees with Kitaigorodski's rule of molecular close packing.[33] The cluster model was created using the atomic coordinates of the γ-glycine neutron structure at 83 K.[17] The vibration frequencies of the glycine molecule in its crystalline environment were calculated with a two-

layer ONIOM model using the program Gaussian03.[34] The central molecule was treated with density functional theory (DFT) at the B3LYP/6-311+G(2d,p) level of theory, the 14 surrounding molecules with the semi-empirical PM3 method. Structural optimization converged rapidly. The same procedure has been satisfactorily applied to the calculation of vibration frequencies of α-glycine,[5,6] β-glycine,[7] and to the modeling of crystalline glycine polymorphs.[35]

4. RESULTS AND DISCUSSION

4.1. Variable-Temperature ADPs. In the absence of phase transformations, the typical ADP curves are smooth and continuous. At high temperatures they show an increase steeper-than-linear, as a consequence of anharmonicity related to thermal expansion. This is what is observed for the ADPs from the KEK data. The positive anharmonic motion is accounted for by a positive Grüneisen parameter (see Fig. 2 and §4.2). In contrast, the temperature evolution of the ADPs based on the ID11 data is linear across the entire temperature range and shows no indication of the expected plateau in the quantum regime between 10 and 100 K (see §4.2). Comparing the ADPs from both sources, the ADPs from ID11 are larger than those from KEK by 3×10^{-3} Å^2 (ca. 15 times their standard uncertainties) for atom O1 at 100 K (Fig. 2b). These differences in ADPs are probably due to the different crystals used, as well as to the different instruments, experimental conditions and different data processing software. Similar differences were noted previously for the ADPs of α-glycine measured at two different synchrotron beamlines (KEK and SPring-8)[5,6] and for β-glycine where the ADPs from synchrotron and sealed tube data[7] differed by as much as 3×10^{-3} Å^2 at 300 K. Close inspection of the ID11 data has revealed that the high intensity reflections at low angles are systematically too weak (see the Wilson plots[36] in Supporting Information, Fig. 3S). This finding could be due to a non-linear response of the detector for high intensities that are still below the saturation level used, however.

4.2. Crystal Dynamics from the ADP Analysis. Three simple normal mode models of motion were fitted to four sets of multi-temperature ADPs with the program NKA:[37] the 'rigid body' model 1 (*rb*) is the simplest model of motion; it considers only molecular librations and translations;[38,39] model 2 (*rbe*) includes contributions from internal vibration in terms of 3 ε tensors: the tensors for the non-H atoms are derived from the ADPs, the tensors for the methylene H-atoms H1, H2 and for the ammonium H-atoms H3, H4, H5 are restrained to the values obtained from the ONIOM calculations; the local coordinate systems of these tensors

are given in the Supporting Information; model 3 (*rbeg*) also includes anharmonic effects accounted for by a single Grüneisen constant. The molecular coordinate system for the normal mode analysis is defined with the *x*-axis along the O1→N1 vector; the *z*-axis is orthogonal to the plane defined by the vectors O1→N1 and C2→C1; the *y*-axis is orthogonal to the *x*- and *z*-axes and completes a right-handed system (Fig. 3). Each of the three models was determined from each of the four ADP sets obtained from the two different sources (KEK and ID11) with two different refinements (IAM and INV). The C–H and N–H distances from X-ray structure determinations are systematically too short as expected; for the ADP analysis the hydrogen atom positions were taken from the neutron structure determinations of γ-glycine[17] to ensure optimal moments of inertia for the librational motion. Although the H-atom isotropic ADPs are included in the normal mode analysis, they affect the models only slightly because their standard uncertainties are large, ~4×10^{-3} Å^2, or ~20 times those of the non-H atoms (Table 2S).

The three models of motion explain the ADPs from the KEK data (Sets 1, 3) better than those from the ID11 data (Sets 2, 4). Here only the model *rbeg* is discussed, which is more theoretically reasonable and gives better goodness-of-fit results (Table 2). The KEK+INV ADPs (Set 1) give a normal positive Grüneisen constant (γ = 2.99) and somewhat more reasonable ε's of the non-H atoms, while the ID11+INV data (Set 2) give an unreasonably large and negative Grüneisen constant (γ = –6.17) and rather larger ε's compared with those from the ONIOM calculations (Table 2). The negative Grüneisen constant is meaningless for glycine because it contradicts the observed positive thermal expansion of the unit cell volume. For both sources, a comparable fit is observed for the ADPs from the IAM and INV refinements respectively, (Sets 1 vs 3; 2 vs 4, Table 2). The more meaningful fit of the *rbeg* model to the KEK+INV data is illustrated by PEANUT[28] difference plots showing small and more or less randomly distributed difference displacements (Fig. 3). For comparison, the PEANUT[28] plots with large and more systematic distributed difference displacements of the ID11+INV data are given in Fig. 4S.

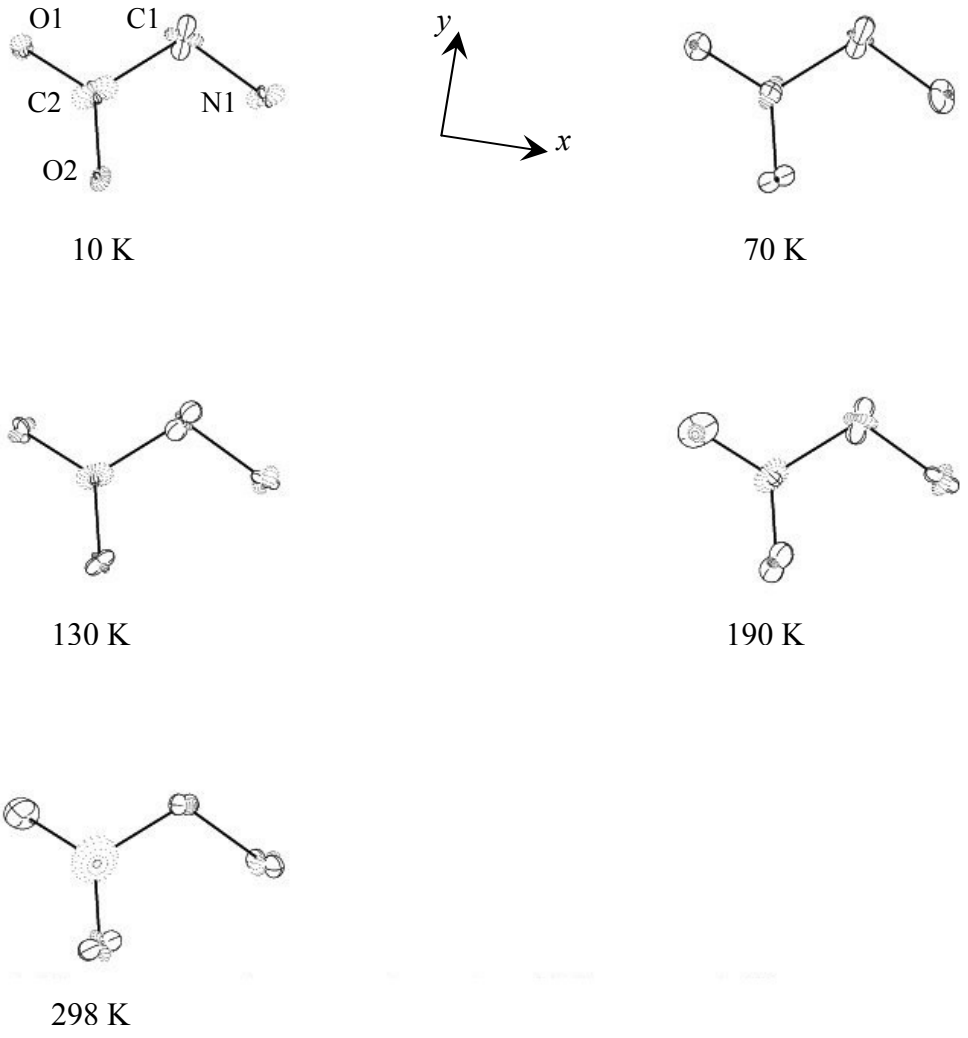

Figure 3. PEANUT[28] plots showing difference displacement parameters $10 \times (U_{obs} - U_{calc})^{1/2}$ of γ-glycine from KEK data (INV refinement, model *rbeg*); positive differences shown with solid lines, negative differences with dotted lines.

Table 2. Normal Mode Analysis of Multitemperature ADPs of γ-Glycine

ADP Set 1: KEK + INV; Model *rbeg*

	frequency $\bar{\nu}$ (cm^{-1}), Grüneisen and eigenvector				ε ($\times 10^{-4}$) [a,b]	GOF	wR_2 (%) [c]
	80.1(0.9)	*64.5(0.6)*	*76.4(0.8)*	*121.6(2.3)*	N1 C1 C2 O1 O2	2.02	5.02
	2.99(0.47)	2.99(0.47)	2.99(0.47)	2.99(0.47)	7(1) 0(1) 1(1)		
L_x	-0.533(33)	-0.232(21)	0.327(55)	-0.646(20)	11(1) 1(1)	observations:	
L_y	-0.265(30)	-0.342(13)	-0.283(28)	0.062(26)	19(2)	175	
L_z	0.406(25)	-0.195(12)	0.205(43)	0.275(22)	H1 H2	restraints: 25	
T_x	-0.568(50)	0.047(18)	0.467(56)	0.673(13)	57 0 0	parameters:	
T_y	-0.258(64)	-0.464(17)	-0.632(29)	0.226(27)	138 0	50	
T_z	0.302(43)	-0.757(15)	0.391(35)	0.003(17)	156		
					H3 H4 H5		
					66 0 0		
					216 0		
					147		

ADP Set 2: ID11 + INV; Model *rbeg*

	68.0(0.8)	*55.7(0.6)*	*66.2(0.8)*	*103.5(2.0)*	N1 C1 C2 O1 O2	2.68	3.94
	-6.17(0.66)	-6.17(0.66)	-6.17(0.66)	-6.17(0.66)	18(1) 1(1) 0(1)		
L_x	-0.598(49)	-0.259(23)	0.275(107)	-0.583(20)	23(1) 4(1)	observations:	
L_y	-0.240(59)	-0.351(13)	-0.337(44)	0.026(21)	27(2)	140	
L_z	0.405(45)	-0.203(13)	0.240(72)	0.268(21)	H1 H2	restraints: 25	
T_x	-0.570(72)	0.059(17)	0.401(100)	0.713(12)	57 0 0	parameters:	
T_y	-0.169(116)	-0.431(16)	-0.658(32)	0.281(24)	138 0	50	
T_z	0.258(73)	-0.761(14)	0.401(49)	0.011(16)	156		
					H3 H4 H5		
					66 0 0		
					216 0		
					147		

ADP Set 3: KEK + IAM; Model *rbeg*

79.8(0.9)	*65.0(0.6)*	*75.5(0.7)*	*119.1(2.2)*		2.36	4.80
2.99(0.45)	2.99(0.45)	2.99(0.45)	2.99(0.45)			

ADP Set 4: ID11 + IAM; Model *rbeg*

69.5(0.8)	*56.5(0.6)*	*66.4(0.8)*	*105.8(2.2)*		2.86	4.46
-5.01(0.64)	-5.01(0.64)	-5.01(0.64)	-5.01(0.64)			

[a] The H-atom epsilons are restrained to the values from ONIOM calculations.
[b] The diagonal elements of epsilon for non-H atoms from ONIOM calculations are 10, 12, 10×10^{-4} Å^2.
[c] $wR_2 = [\sum w(U_{obs} - U_{calc})^2 / \sum w U_{obs}^2]^{1/2}$.

For the small glycine molecule embedded in a network of intermolecular hydrogen bonds and other intermolecular contacts, only the four lowest frequency normal mode frequencies are significantly excited and can be reasonably determined in the limited temperature range of our experiment. The four lattice frequencies from KEK data (64.7, 75.2, 80.3, 121 cm^{-1}; ADP Set 1 in Table 2) are in the range of those from Raman spectroscopy[40–44] (Table 3). A frequency-to-frequency comparison has to be taken with a grain of salt because

the meaning of the frequencies from ADP analysis and spectroscopy is different. Whereas the normal mode frequencies determined from ADPs represent averages over the Brillouin zone and are additionally characterized by eigenvectors, the spectroscopic frequencies refer to the origin of the Brillouin zone and their eigenvectors are generally not known. The frequencies from ADPs are used for estimating the thermodynamic functions in §4.4.

4.3. Internal Vibrations from ONIOM Calculation. The ONIOM(B3LYP/6-311+G(2d,p):PM3) method applied to the 15-molecule cluster of the γ-glycine provides 30 vibrational frequencies (121–3275 cm^{-1}), mainly internal modes (Tables 3S). The average ratio of observed to calculated vibrational frequencies from the 24 highest, mostly molecular deformation modes is 0.992, similar to the scale factors proposed by Scott and Radom.[45] Although the frequencies from the ONIOM calculations and Raman spectroscopy,[43] agree as well as can be expected (Table 4S), the caveat mentioned in §4.2 concerning the comparison of the frequencies and their assignment to specific motions applies here as well. The anisotropic, temperature-independent contributions ε to the ADPs are estimated from the 24 highest ONIOM modes. For the non-H atoms these estimates compare quite well to those from normal mode analysis (Table 2, footnote b); it therefore seems reasonable to constrain the ε's of the H atoms to the calculated values. For an analogous observation and conclusion pertaining to crystalline benzene, see ref. (46).

4.4. Thermodynamic Functions. The four lattice frequencies from the ADP analysis of the KEK data (Table 3) and the 26 highest vibration frequencies from the ONIOM calculation (Table 3S) are used to estimate C_v with the help of the Einstein[9] and Debye[10] models of heat capacity. The difference between $C_p(T)$ and $C_v(T)$ is estimated with the Nernst–Lindemann relation,[11] which is based on the melting temperature (T_m = 519 K for γ-glycine)[47] and a universal constant (1.63×10^{-2} K mol cal^{-1}). In the absence of an experimental value for the compressibility, this relation has been applied successfully earlier to α-glycine,[5,6] polymers and macromolecules.[48] Fig. 4a shows reasonable agreement between C_p from ADP analysis and calorimetry.[1] The small C_p difference of −0.6 cal mol^{-1} K^{-1} at 60 K is probably due to the fact that the lattice frequencies from ADP analysis are a bit lower than those from Raman spectroscopy[40–44] (Table 3). Note that the difference would be even larger if the frequencies derived from the ID11 data had been used. The standard uncertainties of the C_p's from the ADP analysis are calculated by error propagation from the standard uncertainties of the four normal mode frequencies. The uncertainties are in the small percent range and comparable to those from calorimetry:[1] 2–3% for $T < 10$ K; 0.5–1.0% for $10 < T < 50$ K; and 0.04–0.10% for

higher T. The subsequently derived entropies S_{vib} and enthalpies H_{vib} of γ-glycine from ADP analysis are also very similar to those from calorimetry[1] (Fig. 4b).

Table 3. Lattice Vibration Frequencies of γ-Glycine Compared to Those of β- and α-Glycine

	Lattice vib freq (cm^{-1})	Technique	T (K)	Sample	Ref.
γ	64.7, 75.2, 80.3, 121	ADP-analysis on X-ray (KEK)	10–298	Single crystal	This work
	120, 150, 176 [a]	ONIOM(B3LYP/ 6-311+G(2d,p):PM3)	–	Cluster model	This work
	89, 105, 139, 151	Raman spectroscopy	298	Single crystal	40
	41, 91, 105, 154	Raman spectroscopy	300	Polycrystalline	41
	43, 58, 90, 105, 138, 152, 173, 186, 217	Raman spectroscopy	298	Single crystal	42
	89, 104, 138, 152, 170	Raman spectroscopy	298	Single crystal	43
	96, 111, 135, 150, 160	Raman spectroscopy	31	Single crystal	44
β	63.9, 72.0, 80.7, 149	ADP-analysis on X-ray (ID11+BM01A)	10–300	Single crystal	7
	56.2, 96.4, 160, 169 [a]	ONIOM(B3LYP/ 6-311+G(2d,p):PM3)	–	Cluster model	7
	64, 88, 117, 131, 150, 160	Raman spectroscopy	40	Single crystal	44
α	71.3, 77.9, 86.7, 121	ADP-analysis on X-ray (SPring-8) and neutron	18–323	Single crystal	5,6
	144, 154, 166 [a]	ONIOM(B3LYP/ 6-311+G(2d,p):PM3)	–	Cluster model	5,6
	56, 75, 118, 150	Raman spectroscopy	60	Single crystal	44

[a] After scaling with 0.992, 0.974 and 0.982 for the γ-, β- and α-phases, respectively.

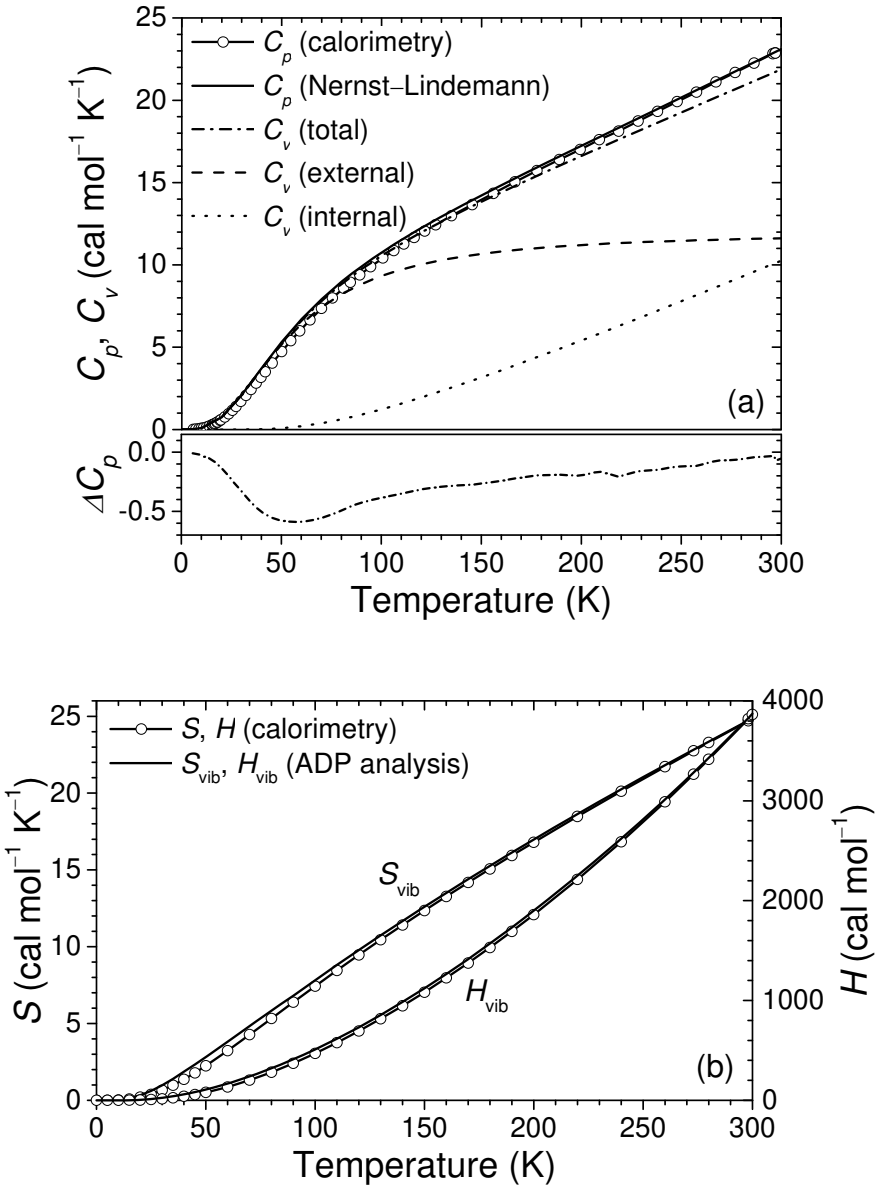

Figure 4. Thermodynamic functions of the γ-glycine polymorph: (a) molar heat capacity and difference ΔC_p = [C_p(calorimetry) – C_p(ADP)]; (b) vibrational entropy and enthalpy (without zero point vibrational energies).

4.5. Relative Thermodynamic Stabilities. *4.5.1. Comparison of Crystal Density and Heat Capacity.* At the macroscopic level, the relative stabilities are sometimes inferred from rules, e.g. the density rule.[49,50] The sequence of calculated crystal densities is β > γ > α with an increment of ≈0.02 g cm^{-3} between polymorphs throughout the temperature range 10–300 K of the diffraction experiments; the density rule asserts that the β-phase is the least stable in agreement with observation, but implies a reversed stability order between the α- and γ-phases in disagreement with the computational and calorimetric data (Fig. 5a).

The differences $\Delta C_p(\mathrm{i}\gamma)$ [= $C_p(\mathrm{i}) - C_p(\gamma)$] obtained from calorimetry and ADP analyses are depicted in Fig. 5b for the temperature range 10–300 K, including the putative β-glycine transition at 252 K,[51] but not the α-γ transition at 396 K.[52] For both techniques, the ΔC_p's are small, the largest difference being < 1.2 cal mol^{-1} K^{-1}. The negative ΔC_p's at 50 < T < 200 K from ADP analysis are probably due to shortcomings of the ADP analysis for γ-glycine at low temperatures; see difference curve in Fig. 4a.

4.5.2. Comparison of Free Energies and Their Components. From a thermodynamic viewpoint, the relative stabilities of the glycine polymorphs depend on the differences of several contributions to the free energy functions $\Delta G(i)$ (i = α, β, γ):

$$\begin{aligned}\Delta G(i) &= E_{lattice}(i) + p\Delta V(i,T) + \Delta H_{ZPE}(i,0\,\mathrm{K}) + \int_0^T C_p(i)dT - T\int_0^T (C_p(i)/T)dT \\ &= \Delta H_{lattice}(i) + \Delta H_{ZPE}(i,0\,\mathrm{K}) + \Delta H_{vib}(i,T) - T\Delta S_{vib}(i,T)\end{aligned} \tag{4}$$

Lattice energies E_{lattice} are available from accurate quantum chemical calculations; their differences may be estimated from sublimation energies. The differences for the glycine polymorphs are small, a few tenth of a kcal mol^{-1}, as may be seen from the most recent and probably most accurate calculations.[53] Differences from other calculations are similar, but may show a different order of stability.[53] The work terms $p\Delta V$, due to thermal expansion, and differences between them are small and negligible in the temperature range of our glycine experiments ($p\Delta V$(γ,300K) = 0.021 cal mol^{-1}; Tables 4 and 4S).

The differences in Zero-Point-Energies, $\Delta\Delta H_{\mathrm{ZPE}}$,[53] are similar to the differences $\Delta E_{\mathrm{lattice}}$, but of opposite sign, thus reducing the stability differences of the polymorphs at 0 K. Note that the sequence of values from DFT calculations and ADP analyses agrees, their order of magnitude is similar, but the differences obtained from quantum calculations are ~300 cal mol^{-1} closer to zero than our estimates, i.e. by an amount that is comparable to the differences in $\Delta E_{\mathrm{lattice}}$, Table 4. To our knowledge the low temperature phonon spectra of the three polymorphs and thus experimental values for ΔH_{ZPE} are not available for comparison.

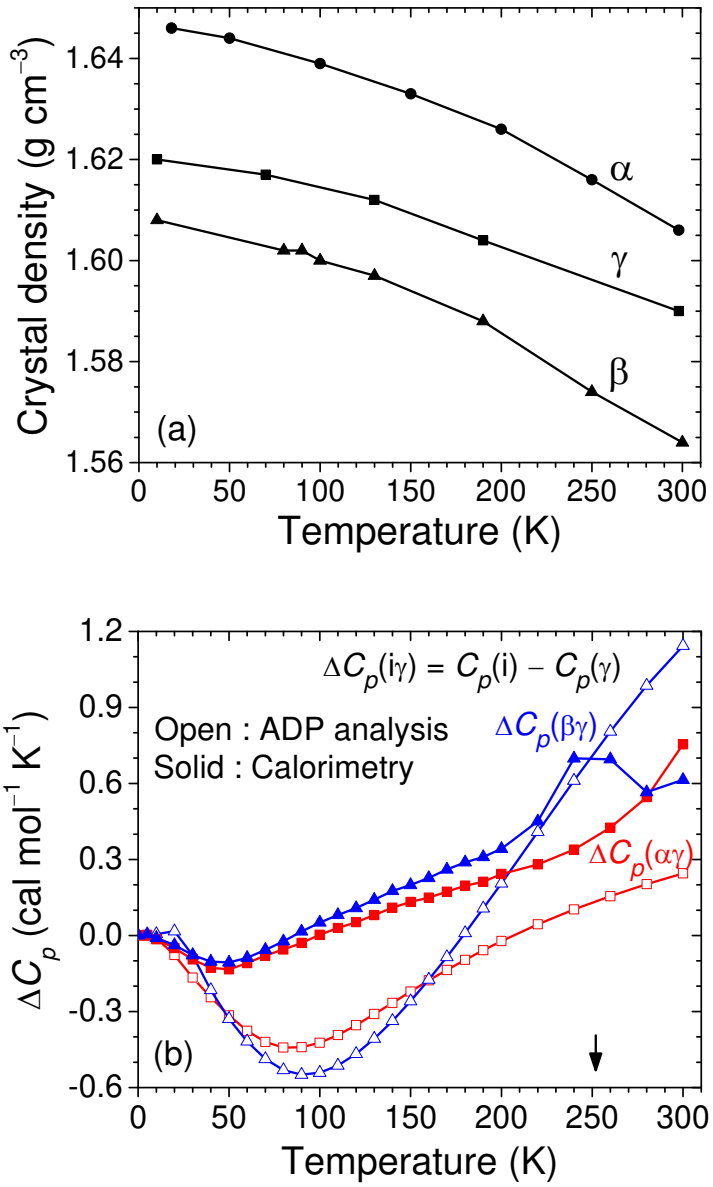

Figure 5. Comparison of (a) calculated crystal densities and (b) molar heat capacities between the three glycine polymorphs; taken from synchrotron data: α, SPring-8;[5,6] β, ESRF;[7] and γ, KEK. The data are given only within the temperature range of this study, well below the melting points of α-glycine at 455 K, of γ-glycine[47] at 519 K and their transition point at 396 K.[52] The putative phase transition at 252 K of β-glycine observed from calorimetry is marked with an arrow.[51]

Table 4. Comparison of Various Contributions to the Enthalpy and Free Energy of the Glycine Polymorphs (in cal mol^{-1}); Standard Uncertainties in Parentheses [a]

	α	β	γ	Ref.
$\Delta E_{\text{lattice}}$	270	580	0	53[b]
$p\Delta V$(300K)	0.003	0.010	0	This work
ΔH_{ZPE}(DFT)	−40	−220	0	53[b]
ΔH_{ZPE}(ADP+ONIOM)	−431	−562	0	This work
$\Delta\Delta H_{\text{vib}}$(calor,298.15K)	48(4)[c]	76(4)[d]	0[e]	1, 51[f]
$\Delta\Delta H_{\text{vib}}$(ADP,300K)	−11(7)	87(7)	0	This work
$-\Delta\Delta H_{\text{dissol}}$(298.15K)	64(27)	142(27)	0	55
$-T\Delta\Delta S_{\text{vib}}$(calor,298.15K)	−22(9)[c]	−71(9)[d]	0[e]	1, 51[f]
$-T\Delta\Delta S_{\text{vib}}$(ADP,300K)	−45(8)	−186(8)	0	This work
$\Delta\Delta G_{\text{vib}}$(calor,298.15K)	26(10)[c]	5(10)[d]	0[e]	1, 51[f]
$\Delta\Delta G_{\text{vib}}$(ADP,300K)	−56(10)	−99(10)	0	This work

[a] Estimated from the square root of the sum of the squared errors; original standard uncertainties are taken from Refs. 1, 51 (calorimetry) and estimated by error propagation from the standard uncertainties of four lattice frequencies (ADP analysis)
[b] see SI of Ref. 53, PBEh+MBD calculation
[c] based on Tab. 3 of Ref. 1
[d] based on Tab. 2 of Ref. 51
[e] based on Tab. 4 of Ref. 1
[f] Note that the differences derived from the summary table 3 of Ref. 51 do not agree with the differences derived from Tab. 3 of Ref. 1, Tab. 2 of Ref. 51 and Tab. 4 of Ref. 1. Here we have chosen to use the latter.

The enthalpic difference $\Delta\Delta H_{\text{vib}}$ are small, but tend to increase the differences between polymorphs. The sum ($\Delta E_{\text{lattice}}$ + ΔH_{ZPE} + $\Delta\Delta H_{\text{vib}}$) is directly comparable to the negative differences in dissolution enthalpies, $-\Delta\Delta H_{\text{dissol}}$.[54] The sums ($\Delta E_{\text{lattice}}$ + ΔH_{ZPE}(DFT) + $\Delta\Delta H_{\text{vib}}$(calor,298.15K) are 278 and 436 cal mol^{-1} for the α- and β-phases respectively, ~200−300 cal mol^{-1} larger than the experimental values but reproducing the observed stability sequence. Replacing ΔH_{ZPE} and the calorimetric value by those estimated from ADP analyses, the calculated differences in dissolution energies are −172(7) and 105(7) cal mol^{-1} making the α-phase slightly more stable than the γ-phase. The discrepancy to the observed stability order may well be a consequence of the experimental difficulties in determining accurate ADPs.

The differences in vibrational entropic contributions, $-T\Delta\Delta S_{\text{vib}}$, are similar in magnitude to the enthalpic differences, but of opposite sign. Therefore the two terms more or less cancel each other suggesting that the vibrational contributions to the free energy differences, $\Delta\Delta G_{\text{vib}}$

= ($\Delta\Delta H_{vib} - T\Delta\Delta S_{vib}$), are not decisive in determining the relative stabilities of the polymorphs.

We conclude that a better understanding of the relative stabilities of the glycine polymorphs requires some improvements of the procedure described here: ΔH_{ZPE} (and $\Delta E_{lattice}$) need to be confirmed, either through experiment or through calculations. With a better understanding of the ZPEs, the estimates of the vibrational enthalpic and entropic contributions are likely to improve as well. The use of periodic DFT calculations seems a promising approach towards a better understanding of polymorph stability.[53,55–57] This conclusion likely holds for polymorphs in general.

5. SUMMARY

This paper completes a series of studies of the three glycine polymorphs aiming at i) analysing the temperature dependence of their ADPs and thus their molecular motion; ii) determining their thermodynamic functions $C_{p,vib}$, ΔH_{vib}, ΔS_{vib} and ΔG_{vib}; and iii) deepening our comprehension of relative polymorph stability.

This paper describes and discusses:

- The measurement and interpretation of variable-temperature synchrotron diffraction data to 0.5 Å between 10 and 300 K for the glycine γ-polymorph. Such data are essential for accurate determination of atomic displacement parameters (ADPs). However, differences in instrumentation, experimental conditions and data processing software resulted in systematic differences in the ADPs obtained from data collected at two synchrotron beam lines. Similar observations apply to the α- and β-polymorphs, albeit to a lesser extent; they show that it is still difficult to obtain multi-temperature diffraction data from synchrotron data that are sufficiently reliable to accurately describe the temperature dependence of ADPs. Present crystallographic data processing programs are largely ‘black box’ objects that are essentially inaccessible to the users. This problem seriously impedes the crystallographic precision experiments needed for the type of study described here.
- As in the studies of the glycine α- and β-polymorphs, the dynamics of the γ-polymorph in the temperature range 10–300 K is described with a model of rigid-body motion including a Grüneisen correction for anharmonic motion and high-frequency intramolecular motion. Four of the 30 vibration frequencies of the glycine molecules in their crystalline

environments have been obtained from ADPs, the remaining 26 from ONIOM calculations (B3LYP/PM3).

- The heat capacities C_v have been estimated from the lattice and internal vibration frequencies with the help of the Einstein and Debye models. C_v has been converted to C_p with the Nernst–Lindemann procedure or with the crystal compressibility if available. From the $C_p(T)$ curves, the thermodynamic functions have been calculated.
- The relative stabilities of the three glycine polymorphs are discussed on the basis of experimental and computational data available in the literature and gathered in our work. Based on comparisons of lattice energies, vibrational zero-point energies, vibrational enthalpies and entropies it is concluded that the most important contributions to the differences in the free energies of the polymorphs are the lattice energies on one hand and the zero point energies on the other. The former requires extremely accurate calculations,[53] the latter a better understanding of the crystal vibrations. Improved high-resolution synchrotron (or neutron) elastic and inelastic diffraction data as well as further, highly accurate quantum chemical calculations will be needed to take this problem a step further. Given our findings for the polymorphs of glycine we suggest that these conclusions may well hold for other groups of polymorphs as well.

ACKNOWLEDGEMENTS

For Part 1, see Aree, T.; Bürgi, H. B. *J. Phys. Chem. A* **2012**, *116*, 8092–8099; Aree, T.; Bürgi, H. B.; Capelli, S.C. *J. Phys. Chem. A* **2012**, *116*, 10037−10037; Part 2, Aree, T.; Bürgi, H. B.; Minkov, V. S.; Boldyreva, E. V.; Chernyshov, D.; Törnroos, K. W. *J. Phys. Chem. A* **2013**, *117*, 8001–8009. This work is supported by the Synchrotron Light Research Institute of Thailand (GRANT 1-2550/PS07). We thank Dr. Loredana Erra at beamline ID11 of the ESRF and Dr. Akiko Nakao of the KEK Photon Factory for help in collecting data and preliminary processing. Help and discussion with Prof. Elena Boldyreva and Dr. Vasily Minkov on crystallization are gratefully acknowledged.

Supporting Information Available:

Information on data collection, data processing, data statistics, figures of unit cell constants, structure factors plots, Wilson plots, normal mode analysis (local coordinate systems for the epsilon tensors; volume expansion; external frequencies and eigenvectors; and PEANUT plots), vibrational frequencies, and table showing the comparison of various contributions to the enthalpy and free energy of the glycine polymorphs. This material is available free of

charge via the Internet at http://pubs.acs.org. Crystallographic information files (CIFs) have been deposited with the Cambridge Crystallographic Data Centre, CCDC nos. 856001–856004 (ID11) and 856005–856009 (KEK). Copies of this information may be obtained free of charge from the Director, Cambridge Crystallographic Data Centre, 12 Union Road, Cambridge CB2 1EZ, UK (fax +44-1223-336033; e-mail deposit@ccdc.cam.ac.uk or via: www.ccdc.cam.ac.uk).

REFERENCES

(1) Drebushchak, V. A.; Kovalevskaya, Yu. A.; Paukov, I. E.; Boldyreva, E. V. Low-Temperature Heat Capacity of α and γ Polymorphs of Glycine. *J. Therm. Anal. Calor.* **2003**, *74*, 109–120.

(2) Iitaka, Y. The Crystal Structure of β-Glycine. *Acta Cryst.* **1960**, *13*, 35–44.

(3) Iitaka, Y. The Crystal Structure of γ-Glycine. *Acta Cryst.* **1958**, *11*, 225–226.

(4) Chilcott, T. C.; Schoenborn, B. P.; Cooke, D. W.; Coster, H. G. L. Anomalous Electrical Behaviour of Single-Crystal Glycine Near Room Temperature. *Phil. Mag. B* **1999**, *79*, 1695–1701.

(5) Aree, T.; Bürgi, H. B. Dynamics and Thermodynamics of Crystalline Polymorphs: α-Glycine, Analysis of Variable-Temperature Atomic Displacement Parameters. *J. Phys. Chem. A* **2012**, *116*, 8092–8099.

(6) Aree, T.; Bürgi, H. B.; Capelli, S.C. Correction to "Dynamics and Thermodynamics of Crystalline Polymorphs: α-Glycine, Analysis of Variable-Temperature Atomic Displacement Parameters. *J. Phys. Chem. A* **2012**, *116*, 10037−10037.

(7) Aree, T.; Bürgi, H. B.; Minkov, V. S.; Boldyreva, E. V.; Chernyshov, D.; Törnroos, K. W. Dynamics and Thermodynamics of Crystalline Polymorphs. 2. β-Glycine, Analysis of Variable-Temperature Atomic Displacement Parameters. *J. Phys. Chem. A* **2013**, *117*, 8001–8009.

(8) Bürgi, H. B.; Capelli, S. C. Dynamics of Molecules in Crystals from Multi-Temperature Anisotropic Displacement Parameters. I. Theory. *Acta Cryst*. **2000**, *A56*, 403–412.

(9) Einstein, A. Plank's Theory of Radiation and the Theory of Specific Heat. *Ann. Phys., Lpz*. **1907**, *22***,** 180–190.

(10) Debye, P. P. Zur Theorie der spezifischen Wärmen. *Ann. Phys., Lpz.* **1912**, *39***,** 789–839.

(11) Nernst, W.; Lindemann, F. A. Specific Heat and Quantum Theory. *Z. Electrochem.* **1911**, 17, 817–827.

(12) Aree, T.; Bürgi, H.-B. Specific Heat of Molecular Crystals from Atomic Mean Square Displacements with the Einstein, Debye, and Nernst−Lindemann Models. *J. Phys. Chem. B* **2006,** *110,* 26129–26134.

(13) Bürgi, H. B.; Capelli, S. C.; Birkedal, H. Anharmonicity in Anisotropic Displacement Parameters. *Acta Cryst*. **2000**, *A56*, 425–435.

(14) Grüneisen, E. Theorie des festen Zustandes einatomiger Elemente. *Ann. Phys., Lpz.* **1912**, *39*, 257–306.

(15) Iitaka, Y. New Form of Glycine. *Proc. Japan Acad.* **1954**, *30*, 109–112.

(16) Kozhin, V. M. Tensors of Thermal Expansion of α-, β-, and γ- Polymorphs of Glycine. *Kristallografiya* (*Sov. Crystallography*) **1978**, *23*, 1211–1215.

(17) Kvick, Å. E; Canning, W. M.; Koetzle, T. F.; Williams, G. J. B. The Crystal Structure of γ-Glycine at 83 K and 298 K by Neutron Diffraction. *Acta Cryst*. **1980**, *B36*, 115–120.

(18) Boldyreva, E. V.; Drebushchak, T. N.; Shutova, E. S. Structural Distortion of the *α*, *β*, and *γ* Polymorphs of Glycine on Cooling. *Z. Kristallogr*. **2003**, *218*, 366–376.

(19) Rousseau, B.; Maes, S. T.; Lenstra, A. T. H. Systematic Intensity Errors and Model Imperfection as the Consequence of Spectral Truncation. *Acta Cryst*. **2000**, *A56*, 300–307.

(20) Weissbuch, I.; Leiserowitz, L.; Lahav, M. "Tailor-Made" and Charge-Transfer Auxiliaries for the Control of the Crystal Polymorphism of Glycine. *Adv. Mater.* **1994**, *6*, 952–956.

(21) Rigaku, *RAPID AUTO*; Version 2.40; Rigaku Corporation: Tokyo Japan, 2006.

(22) Bruker, *SAINT Version 7.34A*; Bruker, AXS Inc., Madison, WI, U. S. A., 2005.

(23) Higashi, T. *ABSCOR*; Rigaku Corporation: Tokyo Japan, 1995.

(24) Sheldrick, G. M. *SADABS Version 2004/1 – Bruker Nonius Program for Area Detector Scaling and Absorption Correction*; University of Göttingen, Germany, 2004.

(25) Bruker, *XPREP Version 2005/2*; Bruker AXS Inc., Madison, Wisconsin, U. S. A., 2004.

(26) Sheldrick, G. M. A Short History of SHELX. *Acta Cryst*. **2008**, *A64*, 112–122.

(27) Prince, E., Ed. *International Tables for Crystallography Vol. C: Mathematical, Physical and Chemical Tables,* 3rd Ed.; Kluwer Academic Publishers: Dordrecht, 2004; pp 554–595.

(28) Hummel, W.; Hauser, J.; Bürgi, H. -B. Peanut: Computer Graphics Program to Represent Atomic Displacement Parameters. *J. Mol. Graphics* **1990**, *8*, 214–220.

(29) Koritsanszky, T.; Howard, S. T.; Richter, T.; Macchi, P.; Volkov, A.; Gatti, C.; Mallinson, P. R.; Farrugia, L. J.; Su, Z.; Hansen, N. K. *XD – A Computer program package for multipole refinement and topological analysis of charge densities from diffraction data*; 2003.

(30) Dittrich, B.; Koritsanszky, P.; Luger, P. A Simple Approach to Nonspherical Electron Densities by Using Invarioms. *Angew. Chem. Int. Ed*. **2004**, *43*, 2718–2721.

(31) Dittrich, B.; Strumpel, M.; Schäfer, M.; Spackman, M. A.; Koritsánszky, T. Invarioms for Improved Absolute Structure Determination of Light-Atom Crystal Structures. *Acta Cryst*. **2006**, *A62*, 217–223.

(32) Hirshfeld, F. L. Can X-ray Data Distinguish Bonding Effects from Vibrational Smearing? *Acta Cryst*. **1976**, *A32*, 239–244.

(33) Kitaigorodski, A. I. *Organic Chemical Crystallography*; Consultants Bureau: New York, 1961.

(34) Frisch, M. J.; Trucks, G. W.; Schlegel, H. B.; Scuseria, G. E.; Robb, M. A.; Cheeseman, J. R.; Montgomery Jr., J. A.; Vreven, T.; Kudin, K. N.; Burant, J. C.; et al. *Gaussian03*, Revision C.02; Gaussian Inc.: Wallingford, CT, 2004.

(35) Peeters, A.; Van Alsenoy, C.; Lenstra, A. T. H.; Geise, H. J. Solids Modeled by Ab Initio Crystal Field Methods. X. Structure of α-Glycine, β-Glycine, and γ-Glycine Using a 15-Molecule Cluster. *J. Chem. Phys*. **1995**, *103*, 6608–6616.

(36) Wilson, A. J. C. The Probability Distribution of X-ray Intensities. *Acta Cryst.* **1949**, *2*, 318–321.

(37) Bürgi, H. -B.; Förtsch, M.; Capelli, S. C.; Hauser, J. *NKA: Program for Normal Coordinate Analysis from Anisotropic Displacement Parameters at Multiple Temperatures*, Version 5.1.16; University of Bern, Switzerland, 2004.

(38) Schomaker, V.; Trueblood, K. N. On the Rigid-Body Motion of Molecules in Crystals. *Acta Cryst*. **1968**, *B24*, 63–76.

(39) Dunitz, J. D.; White, D. N. J. Non-Rigid-Body Thermal-Motion Analysis. *Acta Cryst*. **1973**, *A29*, 93–94.

(40) Hirai, Y.; Nibu, Y.; Shimada, H. Pressure Effect on the Raman Spectra of α- and γ-Glycine Crystals. *Fukuoka University Science Reports* **2005**, *35*, 17–24.

(41) Shi, Y.; Wang, L. J. Colletive vibrational spectra of α- and γ-glycine studied by terahertz and Raman spectroscopy. *Phys. D: Appl. Phys.* **2005**, *38*, 3741–3745.

(42) Balasubramanian, K.; Krishnan, R. S.; Iitaka, Y. Raman Spectrum of γ-Glycine. *Bull. Chem. Soc. Jpn*. **1962**, *35*, 1303–1305.

(43) Baran, J.; Ratajczak H. Polarised IR and Raman Spectra of the γ-Glycine Single Crystal. *Spectrochim. Acta* **2005**, *61A*, 1611–1626.

(44) Surovtsev, N. V.; Malinovsky, V. K.; Boldyreva, E. V. Raman Study of Low-Frequency Modes in Three Glycine Polymorphs. *J. Chem. Phys*. **2011**, *134*, 045102: 1–5.

(45) Scott, A. P.; Radom, L. Harmonic Vibrational Frequencies: An Evaluation of Hartree−Fock, Møller−Plesset, Quadratic Configuration Interaction, Density Functional Theory, and Semiempirical Scale Factors. *J. Phys. Chem.* **1996**, *100*, 16502–16513.

(46) Bürgi, H.-B.; Capelli, S. C.; Goeta, A. E.; Howard, J. A. K.; Spackman, M. A; Yufit, D. S. Electron Distribution and Molecular Motion in Crystalline Benzene: An Accurate Experimental Study Combining CCD X-ray Data on C_6H_6 with Multitemperature Neutron-Diffraction Results on C_6D_6, *Chem. Eur. J.* **2002**, *8*, 3512–3521.

(47) Kumar, R. A.; Vizhi, R. E.; Vijayan, N.; Babu, D. R. Structural, Dielectric and Piezoelectric Properties of Nonlinear Optical γ-Glycine Single Crystals. *Physica B* **2011**, *406*, 2594–2600.

(48) Wunderlich, B. *Thermal Analysis*; Academic Press: Boston, 1990.

(49) Grunenberg, A.; Henck, J. O.; Siesler, H. W. Theoretical Derivation and Practical Application of Energy/Temperature Diagrams as an Instrument in Preformulation Studies of Polymorphic Drug Substances. *Int. J. Pharm*. **1996**, *129*, 147–158.

(50) Bernstein, J. Polymorphism in Molecular Crystals; Oxford University Press: New York, 2002.

(51) Drebushchak, V. A.; Boldyreva, E. V.*;* Kovalevskaya, Yu. A.; Paukov, I. E.; Drebushchak, T. N. Low-Temperature Heat Capacity of β-Glycine and a Phase Transition at 252 K. *J. Therm. Anal. Calor.* **2005**, *79*, 65–70.

(52) Yu, L.; Huang, J.; Jones, K. J. Measuring Free-Energy Difference between Crystal Polymorphs through Eutectic Melting. *J. Phys. Chem. B* **2005,** *109,* 19915–19922.

(53) Marom, N.; DiStasio, R. A.; Atalla, V.; Levchenko, S.; Reilly, A. M.; Chelikowsky, J. R.; Leiserowitz, L.; Tkatchenko, A. Many-Body Dispersion Interactions in Molecular Crystal Polymorphism. *Angew. Chem. Int. Ed.* **2013**, *52*, 6629–6632.

(54) Perlovich, G. L.; Hansen, L. K.; Bauer-Brandl, A. The Polymorphism of Glycine. Thermochemical and Structural Aspects. *J. Therm. Anal. Calor.* **2001**, *66*, 699–715.

(55) Wahlberg, N.; Ciochon, P.; Petricek, V.; Madsen, A. O. Polymorph Stability Prediction: On the Importance of Accurate Structures: A Case Study of Pyrazinamide. *Cryst. Growth Des.* **2014**, *14*, 381–388.

(56) Madsen, A. O.; Civalleri, B.; Ferrabone, M.; Pascale, F.; Erba, A. Anisotropic Displacement Parameters for Molecular Crystals from Periodic Hartree-Fock and Density Functional Theory Calculations. *Acta Cryst.* **2013**, *A69*, 309–321.

(57) Madsen, A. O.; Mattson, R.; Larsen, S. Understanding Thermodynamic Properties at the Molecular Level: Multiple Temperature Charge Density Study of Ribitol and Xylitol. *J. Phys. Chem. A* **2011***, 115*, 7794–7804.

Table of Contents (TOC) Image